# Recompression effects in iris segmentation [*]

Thomas Bergmueller[§†], Eleftherios Christopoulos[†], Martin Schnoell[†]and Andreas Uhl[†]
[†]University of Salzburg, Austria
[§]Authentic Vision, Austria
`tb@authenticvision.com, {echristo, mschnoell, uhl}@cosy.sbg.ac.at`

## Abstract

*Rating a compression algorithm's performance is usually done in experimental studies, where researchers have frequently used JPEG pre-compressed data. It is not clear yet, whether results of such compression experiments are reliable if conducted from pre-compressed data. To investigate this issue, we study the impact of using pre-compressed data on iris segmentation and evaluate the relation between iris segmentation performance and general quality metrics. Furthermore we propose a method to overcome potential problems in case using pre-compressed data sets cannot be avoided, e.g. for reasons of ground-truth availability.*

## 1. Introduction

Iris recognition [3, 22] is one of the most deployed biometric modalities, standardized by the International Civil Aviation Organization (ICAO) for use in future passports, and one of the technologies in the Unique Identification Authority of India's (UID) Aadhaar project to uniquely identify Indian citizens. The increasing market saturation of biometric instead of conventional access control methods raises the need for efficient means to store such data. The International Organization for Standardization (ISO) specifies iris biometric data to be recorded and stored in (raw) image form (ISO/IEC FDIS 19794-6) rather than in extracted templates (e.g. iris-codes). Such deployments benefit from future improvements (e.g. in feature extraction stage) which can be easily incorporated without re-enrollment of registered users. Since biometric templates may depend on patent-registered algorithms, databases of raw images also enable more interoperability and vendor neutrality [22]. These facts motivate detailed investigations and optimisations of image compression on iris biometrics in order to provide an efficient storage and rapid transmission of raw biometric records. Furthermore, the application of low-powered mobile sensors for image acquisition, e.g. mobile phones, raises the need for reducing the amount of transmitted data.

As a consequence, according to the importance of this issue, many studies comparing and optimising lossy compression techniques for iris imagery may be found in the literature. Since the CASIA iris datasets have been very popular among researchers ever since their establishment, many papers dealing with compression have been relying on the (extended) CASIA V1.0 dataset, including also first IREX investigations [21, 13, 17, 9, 14] (apart from other examples using the ICE 2005 dataset [8, 12]).

Since it has been pointed out [20] that the CASIA V1.0 dataset exhibits manipulated pupil areas and should therefore not be used any further in experimentation, compression researchers moved to other (and more recent, more challenging etc.) datasets, e.g. the CASIA V3.0 [11, 22], the CASIA V4.0 [25], the Bath [13, 18], and the UBIRIS.v1 [9, 4] datasets. While the images of CASIA V1.0 and ICE 2005 are given in uncompressed format, images in CASIA V3.0, CASIA V4.0, UBIRIS and Bath datasets are provided as JPEG (the first three) or JPEG2000 (the latter) lossy compressed data. Therefore, any compression experiments conducted on these datasets operate on pre-compressed data. This fact has not been ignored entirely – for example, in [22], preparatory JPEG compression experiments with uncompressed data reveal that slightly pre-compressed data leads to better recognition performance due to denoising effects. Thus experiments with pre-compressed data are assessed to be unproblematic. The same argument is used for JPEG2000 pre-compressed data [18] based on the results in [13]. However, eventual artifacts resulting from recompression effects are not accounted for in these considerations. Recompression artifacts arise in cases where data is compressed twice (or multiple times) with lossy compression schemes, i.e. where artifacts from the first compression step (termed pre-compression) are aggravated or exploited by the second compression step.

Two different types of such effects may be distinguished: First, *intra-recompression*, where the same com-

---

[*] This work has been partially supported by the Austrian Science Fund FWF, project no. P26630.

pression scheme is used several times, whereas in *inter-recompression* different methods are used in the different compression steps. For example, using JPEG pre-compressed data and applying JPEG XR and JPEG2000 [11] or JPEG2000 and fractal compression [4] is eventually prone to inter-recompression artifacts, while the application of JPEG to JPEG pre-compressed data [25, 22] can be prone to intra-recompression artifacts. While next to nothing can be found on the issue of inter-recompression artifacts in the general compression literature, intra-recompression artifacts are better investigated, at least in the case of lossy JPEG compression. Soon after the establishment of the JPEG standard [19], it was found that JPEG recompression artifacts arise and do not follow a linear behaviour [5]. Extensive experiments in this direction can also be found in [15], and following these obversations, requantisation-based schemes have been suggested for JPEG, reducing recompression artifacts considerably [1]. Recently, the identification of images which underwent JPEG double compression (i.e. JPEG intra-recompression) has been a hot topic in image forensics [24]. Taking all these facts together, it gets clear that recompression artifacts may impact experimental results with respect to biometric recognition performance, an issue, that has been neglected so far. As discussed, ISO/IEC FDIS 19794-6 requires storing biometric data as raw images, hence all components of a biometric system are affected when operating with compressed data. As we investigate the recompression issue by studying impact on an iris recognition system, the influence on segmentation and texture extraction as well as feature extraction, i.e. iris code computation, has to be evaluated. [23, 8] suggest that data reduction has the highest impact on the iris segmentation. Since segmentation is also the first step in the pipeline, this potentially effects the performance of later steps as well and is therefore of particular importance.

We systematically investigate eventual intra- and inter-recompression effects in an experimental study for iris segmentation. Given the importance of JPEG (as the CASIA V3.0/V4.0 and UBIRIS.v1 datasets are only available in this format), we focus on JPEG pre-compressed data. In our experiments, we compare iris segmentation and general purpose image quality metrics applied to single compressed vs. recompressed (i.e. JPEG pre-compressed) iris image data. Section 2 discusses relevant aspects on generating single- and recompressed data. The used data sets and methods are described in section 3. Section 4 introduces several experiments and lists their results, which are then compared in section 5. From the experiments' individual and comparison results, we draw conclusions in section 6.

## 2. Compression scheme

As discussed, we investigate whether there is a difference in using truly uncompressed data or pre-compressed data in experiments rating the performance of an iris segmentation. Using pre-compressed data means a pre-compressed image $I_p$ is compressed a second time, resulting in an recompressed image $I_r$. When compressing a truly uncompressed image $I_u$, the resulting image $I_s$ is generated in a single compression step. Since experiments are typically carried out on a data set with more than one image, we denote $I_u^{(k)}, I_p^{(k)}, I_s^{(k)}, I_r^{(k)} \in \mathbb{R}^{w \times h}$ as the $k^{th}$ image with width $w$ and height $h$. For simplicity, $I_u, I_p, I_r, I_s$ subsequently denote a particular image but unspecified image of a data set. Furthermore, we define $s(F) \in \mathbb{N}$ with $F \sim I \in \mathbb{R}^{w \times h}$ as a function that returns the file size of the file $F$ storing an image $I$. Since common lossy compression algorithms also employ lossless compression methods, e.g. run-length encoding, before writing to a file, $F$ is only loosely related to the pixel data, namely the image, $I$. For simplicity, we denote $s(I)$ as the file size of the file $F$ encoding the pixel values of an image $I$. $c_m(I, q)$ with $q \in \mathbb{N}$ describes the process of compressing an image $I$ using a particular method $m$ parametrized with the quality parameter $p$. In terms of this paper we use the values $m \in \{jpg, jxr, j2k\}$, where

- $jpg$ corresponds to the well-known (ISO/IEC IS 10918-1) DCT-based image compression method JPEG,
- $j2k$ corresponds to the wavelet-based image compression standard JPEG2000 (ISO/IEC IS 15444-1), which can operate at higher compression ratios and
- $jxr$ corresponds to a compression standard JPEG-XR based on Microsofts HD Photo, which is specified in (ISO/IEC IS 29199-2).

For rating an image $I$'s compression effectiveness, we define the compression ratio $cr$ between an uncompressed image $I_u$ and a compressed image $I_c$ as

$$cr(I_u, I_c) = \frac{s(I_u)}{s(I_c)} \quad \text{with} \quad I_c \in \{I_r, I_s\} \tag{1}$$

For the later described experiments, images are compressed to a target compression ratio $cr_t \in \mathbb{R}$. However, only the *j2k* compression standard allows to specify a target compression ratio $cr_t$ directly via parameter $q$. Hence this is the only method where we can control the file size $s(I_c)$ directly. The other two compression methods take a quality parameter $q \in \mathbb{N}$ only, controlling the quality but not the file size $s(I_c)$. Thus it is not possible to set this parameter to meet a certain target compression ratio $cr_t$. Due to the quality parameter's limited set of quality parameters, the target compression ratio $cr_t$ cannot be achieved exactly for any of the three methods. Parameter optimisation can be done, such that $cr_t \approxeq cr(I_u^{(k)}, I_c^{(k)})$. We propose an algorithm to compress a set of $K$ uncompressed images $I_u$

using a particular method $m$ to achieve a certain compression ratio $cr_t$ in a way that the compression ratio of each image is met as close as possible. This process, illustrated in Fig. 1, employs

1. Compute the single-compressed image $I_s^{(k)}$ with method $m$ such that $cr(I_u^{(k)}, I_s^{(k)}) \approx cr_t$. The optimal quality parameter $q_s^{(k)}$ is computed for each image separately by
$$s_t^{(k)} = \frac{s(I_u^{(k)})}{cr_t} \tag{2}$$
$$q_s^{(k)} = \underset{q\in\mathbb{N}}{argmin} |s(c_m(I_u^{(k)}, q)) - s_t^{(k)}|, \tag{3}$$
where $s_t^{(k)}$ is the file size exactly meeting the target compression ratio $cr_t$. This is implemented by iteratively searching the quality parameter $q$ that results in the closest achievable compression ratio $cr(I_u, I_c)$. The single compressed images $I_s^{(k)}$ using method $m$ are computed with the optimal parameters $q_s^{(k)}$ as
$$I_s^{(k)} = c_m(I_u^{(k)}, q_s^{(k)}) \tag{4}$$
2. Compute a pre-compressed image $I_p^{(k)}$ using $jpg$-method with an arbitrary but fixed quality parameter $q_p$, i.e.
$$I_p^{(k)} = c_{jpg}(I_u^{(k)}, q_p) \tag{5}$$
3. Now, find a quality parameter $q_d^{(k)}$ that allows to compress the pre-compressed image $I_p^{(k)}$ a second time, such that the resulting recompressed image $I_r^{(k)}$ has the same file size as the single-compressed image $I_s^{(k)}$, i.e. $s(I_s^{(k)}) \approxeq s(I_r^{(k)})$. Such a quality parameter $q_r^{(k)}$ can be found by optimising
$$q_r^{(k)} = \underset{q\in\mathbb{N}}{argmin} |s(c_m(I_p^{(k)}, q)) - s(I_s^{(k)})| \tag{6}$$
$$\forall s(I_s^{(k)}) \geq s(I_r^{(k)}) \tag{7}$$
The condition $s(I_s^{(k)}) \geq s(I_r^{(k)})$ is of importance to establish fair conditions, since it is very likely that the file sizes $s(I_s^{(k)}), s(I_r^{(k)})$ cannot be equalized due to the limited set of the quality parameters $q$. The recompressed images $I_r^{(k)}$ are then computed from the pre-compressed images $I_p^{(k)}$ with the found optimal parameters $q_r$ as
$$I_r^{(k)} = c_m(I_p^{(k)}, q_r^{(k)}) \tag{8}$$

Using data sets generated with this method, we can investigate the impact of artifacts in an recompressed image $I_r$ in comparison to those in single-images $I_s$. The first one contains artifacts by two compression, while the latter one contains artifacts from one compression step only.

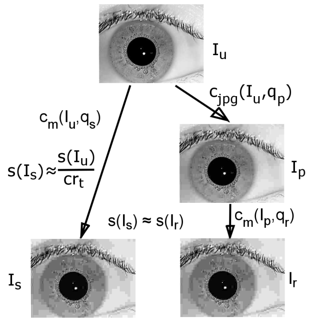

Figure 1. Compression principle to obtain two images achieving approximately the same target compression ratio $cr_t$ from an uncompressed image $I_u^{(k)}$ using a particular compression method $m$. One image, $I_s^{(k)}$, is compressed in a single step while the other, $I_r^{(k)}$, uses a pre-compression and a final compression step. The pre-compression step is always a $jpg$-compression, while the final one uses the same method $m$ as used in single-compression.

## 3. Experimental setup

Although there are several iris data sets around, few are available in uncompressed format. We use the IITD Iris data base[1]. The main reason for this is the availability of a segmentation ground truth created by an expert, which was recently introduced by Hofbauer *et al.* [10] and used in [23]. The $k^{th}$ image of this segmentation ground truth data set is subsequently denoted as $SGT^{(k)}$. According to information by the IITD iris data base's authors, the images, stored in a 3-channel uncompressed bitmap format[2] are already JPEG-compressed with 100% quality by the sensor (JIRIS, JPC1000). Since they are stored as bitmaps, all images have an identical file size of $s(I_u)$=230,454 bytes. Despite not being optimal, using the IITD was necessary due to the available ground truth, for reasons becoming obvious in section 4.2. Futhermore, the IITD – contrary to others, e.g. the ND-IRIS-0405 iris image dataset [2] – is captured under favorable conditions, which allows for lower segmentation errors. This is necessary to distinguish between noise and recompression-effects. We use the scheme introduced in section 2 to compress obtain data sets with target compression ratios $cr_t \in \{15, 20, 25, ..., 70, 75\}$. For each of these target compression ratios $cr_t$, the pre-compression step in recompression mode is carried out with quality parameters $q_p \in \{100, 80, 75, 70\}$ to simulate different levels of pre-compression. Each of these combinations is used to compress with the introduced $jpg$, $j2k$ and $jxr$ methods. We start at compression ratio $cr_t = 15$, because

---

[1] IITD Iris Database version 1.0, www4.comp.polyu.edu.hk/˜csajaykr/IITD/Database_Iris.htm

[2] We want to point out that storing in 1-channel bitmaps would be more efficient, since the images were captured in near-infrared. However, we use the size information of the 3-channel bitmap in computing compression ratios

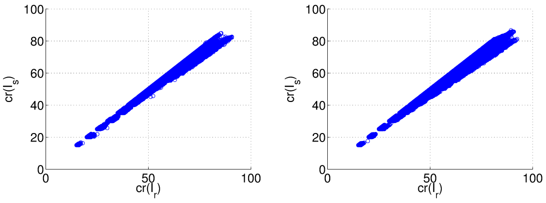

|  | single: $1 - \frac{cr(I_u,I_s)}{cr_t}$ |  |  | recomp.: $1 - \frac{cr(I_u,I_r)}{cr_t}$ |  |  |
|---|---|---|---|---|---|---|
| **%** | *jpg* | *j2k* | *jxr* | *jpg* | *j2k* | *jxr* |
| $\mu$ | -3.21 | -3.48 | -4.33 | -6.80 | -7.04 | -9.49 |
| $\sigma$ | 2.74 | 2.51 | 2.87 | 4.83 | 4.23 | 4.34 |

Figure 2. Scatter plots of measured compression ratios $cr(I_u, I_s)$ over $cr(I_u, I_r)$ for methods *jpg* (left) and *jxr* (right). The graphs indicate that the $s(I_s^{(k)}) \geq s(I_r^{(k)})$ condition from equ. (7) is satisfied. While this is indeed true for *j2k* and *jxr*, we observe a violation in 0.13% of the cases for *jpg* at $cr_t \geq 70$, because JPEG is already working at it's boundaries at such high compression ratios. The table below reveals, that in average the aimed $cr_t$ is met with 3.67% accuracy for single-compressed images $I_s$, while the recompressed ones $I_r$ only reach 7.8%. This is due to the limited set of quality parameters $q, q_p$.

even a pre-compression with $q_p = 100$ achieves - depending on the image's content - already a compression ratio of $cr(I_u, I_p) \approx 10$. For obvious reasons, no smaller compression ratio $cr(I_u, I_r) < cr(I_u, I_p)$ can be reached in recompression. This results in a total of 195 data sets with 2240 images each, whose distribution is shown and discussed in fig. 2.

## 4. Evaluation

We investigate the behavior of iris segmentation employing a segmentation error rate (section 4.2). Besides that, we assess the image quality with fully-referenced metrics (section 4.1). The individual results are then compared in 5.

### 4.1. Full-referenced quality metrics

Evaluating the quality of the compressed images in respect to the original an assortment of full-reference metrics was chosen. The choice was made according to different aspects of human perception starting from mathematically defined to low-level features based and finally to high-level features based. The following were included:

- PSNR: Peak signal-to-noise ratio.
- MSSIM[26]: Multi-scale structural similarity index is an extension of the SSIM metric. After the extraction of luminance, structure and contrast components from the image at scale 1, the algorithm iteratively applies a low pass filter and downsamples the filtered image by a factor of 2. The overall result is the combination of measurements at different scales.
- NQM[7]: Noise Quality Measure, a low-level HVS features based metric. The contrast pyramid of Pelis work was used to model the variation in contrast, sensitivity with distance, dimensions and spatial frequency of the stimuli, and with the variation of their local luminance mean.
- RFSIM[16]: Riesz-transform feature based similarity metric approximates HVS by perceiving an image mainly according to its low-level features and uses the 1st-order and 2nd-order Riesz transform coefficients. The similarity index is measured by comparing the two feature maps at key locations marked by the feature mask. The mask is generated by a Canny operator.
- VSNR[6]: Visual Signal-to-Noise Ratio, a wavelet based metric. The metric is designed to evaluate both low-level and mid-level HVS features. VSNR works in two stages: The first computes the contrast detection thresholds, while the second estimates visual fidelity by measuring the perceived contrast and the extent to which the distortions disrupt global precedence.

Applying these quality metrics *jpg*, *j2k* and *jxr* resulted in the following observations in figure 3 and 4. It is observed that:

1. For *jpg* and $cr_t > 15$ single compressed images were of higher quality compared to recompressed ones and at $cr_t$=15 the single compressed images were of the lowest quality as shown in figure 3 for MSSIM. The quality of the recompressed images followed the trend that the higher the $q_p$ the better the quality of the image. Previous observation of metrics for jpg was unanimous for all metrics.
2. For *jk2* in all compression ratios and all metrics, the quality of the recompressed images followed the trend that the higher the $q_p$ the better the quality of the image. Single compressed images were of the highest quality compared to recompressed data, which was valid for all metrics and compression ratios as shown for MSSIM in fig. 3.
3. For *jxr* and $15 \leq cr_t \leq 40$ single compressed images were of the lowest quality compared to recompressed data for MSSIM and VSNR. The latter followed the trend of the higher the $q_p$ the better the quality of the image (fig. 4). For $45 \leq cr_t \leq 75$ images of single compression became of the highest quality and recompressed data continued the same trend for MSSIM and VSNR metrics. NQM showed the same behaviour, but $cr_t$=50 was observed to be the changing point in this case. RFSIM showed a different trend from the previous; single compressed data were always of the

best quality compared to recompressed data which followed in terms of quality measurement.

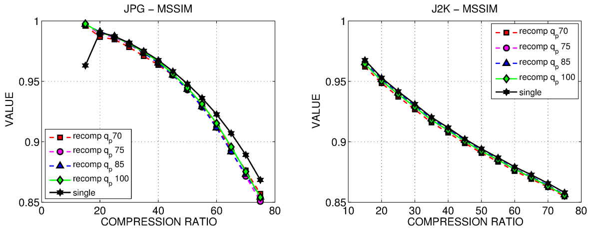

Figure 3. Left: MSSIM of *jpg* single- and recompressed data. Right: MSSIM of *j2k* single- and recompressed data

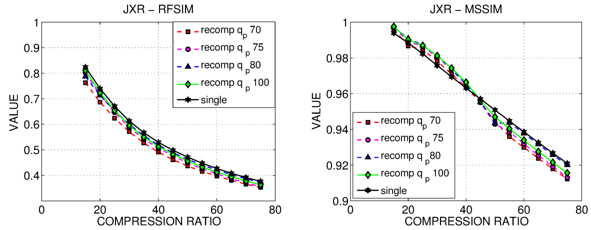

Figure 4. Left: RFSIM of *jxr* single- and recompressed data. Right: MSSIM of *jxr* single- and recompressed data

## 4.2. Segmentation error rates

In iris recognition, the segmentation of an iris image is considered as one of the most critical parts [8, 23]. We investigate the differences of single- and recompression as well as the aspects of which reference to use. We distinguish between using an absolute reference, e.g. a ground truth, and a relative one, e.g. the segmentation of the uncompressed images $I_u$, when computing the error rate.

The segmentation accuracy is rated by the mean segmentation error rate, which corresponds to the suggested E1 error rate in the Noisy Iris Challenge Evaluation - Part I (NICE.I). We define the segmentation error rate $ser$ as

$$ser(R,S) = \overline{R \oplus S} \in [0,1] \quad with \quad R,S \in \{0,1\}^{w\times h}, \tag{9}$$

where $R$ is the binarized reference segmentation and $S$ the binarized segmentation result of the same image $I$. The

Figure 5. Segmentation masks of the expert ground truth [10], relative groundtruth $seg(I_u^{(k)})$ and an actual segmentation result $seg(I_r^{(k)})$ (f.l.t.r)

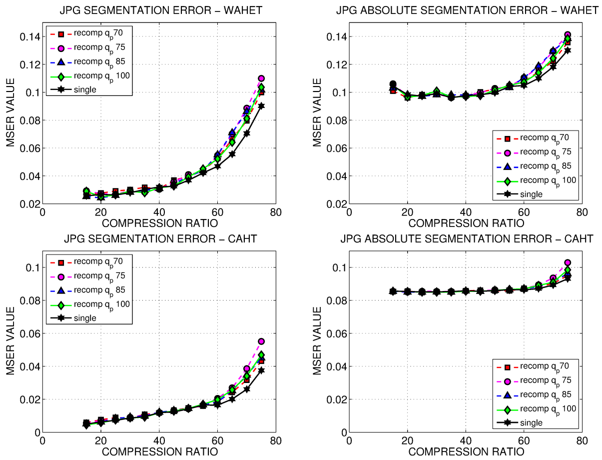

Figure 6. Relative and absolute segmentation error $mser_{rel}$ (left) and $mser_{abs}$ (right) with WAHET (top) and CAHT (bottom) segmentation on $jpg$-compressed data. Note that the $mser_{abs}$ is generally higher than $mser_{rel}$, because the tested algorithms ignore eyelids, yet they are considered in the expert ground truth [23].

mean value of the pixel-wise exclusive-or is the percentage of pixels different in the segmented image $S$ in respect to the reference $R$. Due to multiple images in a data base, the mean segmentation error $mser$ is computed from $K$ images. We compute the absolute mean segmentation error $mser_{abs}$ in respect to the ground truth $SGT$ and the relative mean segmentation error $mser_{rel}$ in respect to the segmentation of the uncompressed images $I_u$ for single- and recompressed images $I_c \in I_s, I_r$. By denoting the segmentation result of an image $I$ as $seg(I) \in \{0,1\}^{w\times h}$ we have

$$mser_{abs} = \frac{1}{K}\sum_{k=1}^{K} ser(SGT^{(k)}, seg(I_c^{(k)})) \tag{10}$$

$$mser_{rel} = \frac{1}{K}\sum_{k=1}^{K} ser(seg(I_u^{(k)}), seg(I_c^{(k)})) \tag{11}$$

The absolute segmentation error rate is considered to be optimal because of the available ground truth. However, for most data bases no such ground truth is available. Therefore we evaluate if the same conclusions as from the $mser_{abs}$ can be drawn from the $mser_{rel}$. The benefit of such a relation (if it exists) is that the $mser_{rel}$ can be computed for any arbitrary data set.

The data set described in section 3 is used to test the two iris segmentation algorithms, Contrast-adjusted Hough Transform (CAHT) and Weighted Adaptive Hough and Ellipsopolar Transform (WAHET), from the USIT Framework v1.0.3[3].The behaviour of these algorithms in respect to compression and impact of other artifacts is already anal-

---

[3] as available at `http://wavelab.at/sources/` [22]

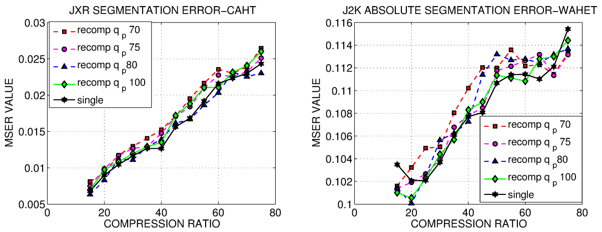

Figure 7. Relative CAHT segmentation error rate $mser_{rel}$ for *jxr*-compressed data (left) and absolute WAHET segmentation error rate $mser_{abs}$ for *j2k*-compressed data (right)

ysed in literature [23, 22]. From the results we observe the following:

1. Results for intra-recompression experiments, namely *jpg* on *jpg* pre-compressed data, in figure 6 indicate:

   (a) For small and medium compression ratios ($cr_t \leq 50$) no significant difference in segmentation errors of single- and recompressed data is observeable. This implies that for these compression ratios it has no impact whether pre-compressed or uncompressed data is used in experiments.

   (b) For large compression ratios ($cr_t > 50$), segmentation errors tend to be lower for single-compressed data compared to recompressed data. Thus using pre-compressed or uncompressed data in experiments matters.

   (c) $mser_{rel}$ and $mser_{abs}$ generally show the similar trends for medium and large compression ratios, i.e. there is a strong correlation of $mser_{rel}$ and $mser_{abs}$ for $cr_t > 30$. This means, the relative error $mser_{rel}$ suffices to rate performance on iris segmentation here, implying no expert-generated ground truth is needed.

   (d) However, WAHET segmentation errors reveal that in some cases there can be a difference between $mser_{rel}$ and $mser_{abs}$ for $cr_t \leq 30$. Figure 6 shows here a different behaviour between absolute error $mser_{abs}$ (top-right) and relative error $mser_{rel}$ (top-left). Hence, for low compression ratios a ground truth is required.

   (e) In recompression, one might expect a linear relation between used pre-compression quality $q_p$ and ranking of the error rates. Interestingly, when looking at figure 6 at high compression ratios, the poorest performance corresponds to $q_p = 75$, while the best is related to $q_p = 70$. In contradiction, $q_p = 100$ performs significantly better than $q_p = 80$ in most settings.

2. There are no clear trends for inter-recompression experiments, namely *jxr* or *j2k* on *jpg* pre-compressed data. Even so, some interesting observations are made, which are illustrated figure 7:

   (a) Data generated in a single compression step generally tends to result in smaller error rates compared to those computed from recompressed data. Interestingly, for extreme values, namely very small and very large compression ratios, single-compression performs often poorer.

   (b) For all experiments carried out with *jxr* and *j2k*, the error rate flattens in some way for medium compression ratios, i.e. $45 \leq cr_t \leq 70$. As an example this can be seen in the $mser_{abs}$ for *j2k*-method (figure 7 left). The characteristics of a curve's flattening vary depending on the pre-compression quality $q_p$. Since flattening can be seen in single- as well as recompressed data, we conclude the effect is generally related to the used methods *jxr* and *j2k*. However, the characteristics of the flattening seem be controlled by the pre-compression quality $q_p$ in a way that the lower the pre-compression quality is, the clearer the curve stagnates.

**In (jpg) intra-recompression,** recompression effects have a strong impact on experimental results for large compression ratios, i.e. $cr_t > 50$ (1a, 1b). Researchers are often forced to use precompressed data sets for the sake of ground truth availability. Results for compression ratios of $cr_t > 50$ can therefore not be considered entirely reliable (1b). However, recompression effects have negative influence on segmentation error rates, hence by using uncompressed data for the same experiments, better results may be achieved. If this behaviour is related to intra-recompression in general or for *jpg*-recompression only, is topic to further research.

From 1c we know that for large compression ratios, i.e. $cr_t > 50$, there is no difference in the progress of $mser_{rel}$ and $mser_{abs}$. Since this is (from 1b) exactly the range, where using single- or recompressed data does have an impact, we propose - based on observations 1d and 1c - to bench-mark compression algorithms in respect to iris segmentation by using

- uncompressed data sets rated with relative measures, such as the $mser_{rel}$, for severe compression, i.e. $cr_t > 50$ and

- pre-compressed data sets[4] with absolute measures, such as $mser_{abs}$, for medium and light compression, i.e. $cr_t \leq 50$.

---

[4] If absolutely necessary because of ground-truth availability, of course uncompressed data is preferred

If this applies to intra-recompression with other methods as well needs further investigation.

**In inter-recompression** we cannot observe such behaviour. However, there are trends observeable (2a, 2b), which need further investigation.

## 5. Comparison

Besides evaluating the segmentation error rate and the general purpose quality measures independently, their correlation is analysed. Furthermore, we explicitly investigate the correlation between $mser_{rel}$ and $mser_{abs}$ to back up the observations in section 4.2. For this purpose, we used the Spearman's rank correlation coefficient (SRCC).

In general, all five used general purpose quality metrics show a high linear relationship with a minimum SRCC of 0.852 to each other. Furthermore, all of these metrics are highly correlating with the segmentation error rate and there are only minor differences between the segmentation algorithms (WAHET and CAHT) and the relative and absolute segmentation error rates. Table 1 shows the correlation results for the intra-recompression (*jpg*) and the CAHT segmentation algorithm. It can be observed that the $mser_{rel}$ shows overall a higher linear relationship to the quality metrics than the $mser_{abs}$. The reason for this can be seen in Figure 6 (bottom) where the $mser_{rel}$ has a higher slope for small and medium CRs where the $mser_{abs}$ is more flat in this region and is in general more noisy as well. Furthermore, it can be seen that for the MSSIM metric ($mser_{rel}$) in case of single compression the SRCC is smaller compared to the other metrics, which is due to the outlier of the MSSIM at $cr_t = 15$ in Figure 3. However, except of this outlier, the MSSIM outperforms the other four quality metrics and in general represents the segmentation error rates best. In case of the intra-recompression the MSSIM agrees clearest with the already in section 4.2 (1b) observed trend that for $cr_t > 50$ the MSER of the single-compressed data shows a lower error and therefore a higher quality than the recompressed data. In case of the inter-recompression for j2k, however, no quality metric describes the behaviour of the MSER well. Figure 7 shows here the best example and clearly differs from the MSSIM graph in Figure 3. For the jxr compression, MSSIM is again the best choice in representing the segmentation error rates since it shows the most linear behaviour and therefore correlates better with the $mser_{rel}$ in Figure 7 than the other metrics. So in general, MSSIM outperforms the other general purpose quality metrics and agrees with the global trend of the segmentation error rates. However, this metric might be not a sufficient choice in all scenarios, especially if a metric should describe more detailed behaviour than just the global trend of iris segmentation as it could be observed in the j2k inter-recompression.

| | *single* | *rec.70* | *rec.75* | *rec.80* | *rec.100* |
|---|---|---|---|---|---|
| *PSNR* | -0.995 | -0.995 | -1.0 | -1.0 | -1.0 |
| *MSSIM* | -0.912 | -0.995 | -1.0 | -1.0 | -1.0 |
| *NQM* | -0.995 | -0.995 | -1.0 | -1.0 | -1.0 |
| *VSNR* | -0.995 | -0.995 | -1.0 | -1.0 | -1.0 |
| *RFSIM* | -0.995 | -0.995 | -1.0 | -1.0 | -0.995 |

| | *single* | *rec.70* | *rec.75* | *rec.80* | *rec.100* |
|---|---|---|---|---|---|
| *PSNR* | -0.857 | -0.863 | -0.929 | -0.868 | -0.841 |
| *MSSIM* | -0.923 | -0.863 | -0.929 | -0.868 | -0.841 |
| *NQM* | -0.857 | -0.863 | -0.929 | -0.868 | -0.841 |
| *VSNR* | -0.857 | -0.863 | -0.929 | -0.868 | -0.841 |
| *RFSIM* | -0.857 | -0.863 | -0.929 | -0.868 | -0.846 |

Table 1. Spearman Rank Correlation Coefficient between quality metrics and $mser_{rel}$ (above) as well as $mser_{abs}$ (below) for intra-recompression (*jpg*) and the CAHT segmentation.

| | *single* | *rec.70* | *rec.75* | *rec.80* | *rec.100* |
|---|---|---|---|---|---|
| *jpg* | 0.703 | 0.835 | 0.890 | 0.786 | 0.863 |
| *j2k* | 0.978 | 0.962 | 0.978 | 0.923 | 0.978 |
| *jxr* | 0.742 | 0.956 | 0.423 | 0.544 | 0.412 |
| | *single* | *rec.70* | *rec.75* | *rec.80* | *rec.100* |
| *jpg* | 0.863 | 0.802 | 0.928 | 0.868 | 0.841 |
| *j2k* | 0.984 | 1.0 | 0.995 | 1.0 | 1.0 |
| *jxr* | 0.978 | 0.973 | 0.967 | 0.918 | 0.978 |

Table 2. SRCC between $mser_{rel}$ and $mser_{abs}$ for all three methods and both WAHET segmentation (above) and CAHT segmentation (below).

The SRCC between the relative and absolute segmentation error rates confirms that both metrics have the same trend as it can be seen in Table 2. In case of the WAHET segmentation *j2k* outperforms the other two compression methods. The smaller SRCC values for *jpg* is mainly due to the $mser_{abs}$ at smaller compression ratios where the segmentation error rate is higher for $cr_t = 15$ than for $cr_t = 20$. Also the small ripple at $cr_t = 30$ has an impact on the correlation here. The reason for the intermediate SRCC results in case of jxr are mainly due to noise.

## 6. Conclusion

Often researchers use JPEG pre-compressed data for iris biometrics compression performance testing in experimental experiments, mostly because of ground-truth availability. We investigated whether the outcome of such experiments can be considered reliable by comparing segmentation error and quality metrics of single-compressed and re-compressed data. In the segmentation error rate, no tendency is observeable when comparing single-compression and inter-recompressed data. However, using intra-recompressed data, i.e. compressing JPEG pre-compressed data with JPEG again, a different behaviour is observed for high compression ratios compared to single-compressed data sets. Thus results of studies using JPEG compression on JPEG pre-compressed data cannot be considered entirely reliable. We showed for small compression ratios, a ground truth is indeed necessary for accurate segmentation error rating. We also propose a method to overcome such problems in section 4.2. Interestingly, there is no strictly linear relation between image quality and segmentation error rate. Quality metrics tend to omit detailed behavior of the segmentation error in respect to compression ratios. Nevertheless, quality metrics and segmentation error follow the same trends and quality metrics can therefore be used to estimate an iris segmentation algorithms behavior.

So far only the impact on two iris segmentation algorithms has been considered. Recompression artifacts potentially influence different algorithms and other parts of an iris recognition system as well. This is topic to further research.

## References

[1] H. Bauschke, C. Hamilton, M. Macklem, J. S. McMichael, and N. Steward. Recompression of jpeg images by requantization. *IEEE Transactions on Image Processing*, 12(7):843–849, 2003.

[2] K. W. Bowyer and P. J. Flynn. The nd-iris-0405 iris image dataset. Technical report.

[3] M. Burge and K. Bowyer, editors. *Handbook of Iris Recognition*. 2013.

[4] M. Carneiro, A. Veiga, E. Flores, and G. Carrijo. Solutions for iris segmentation. In Z. Riaz, editor, *Biometric Systems, Design and Applications*, pages 111–128. InTech, 2011.

[5] S. Chan. Recompression of still images. Technical Report 21068, Computing Laboratory, University of Kent, UK, 1992.

[6] D. M. Chandler and S. Hemami. Vsnr: A wavelet-based visual signal-to-noise ratio for natural images. *IEEE Transactions on Image Processing*, vol. 16, no. 9:pp. 2284–2298, 2007.

[7] N. Damera-Venkata, T. D. Kite, W. S. Geisler, B. L. Evans, and A. C. Bovik. Image quality assessment on a degradation model. *IEEE Transactions on Image Processing, vol. 9, no. 4, pp. 636-649*, 2000.

[8] J. Daugman and C. Downing. Effect of severe image compression on iris recognition performance. *IEEE Transactions on Information Forensics and Security*, 3, 2008.

[9] J. Hämmerle-Uhl, C. Prähauser, T. Starzacher, and A. Uhl. Improving compressed iris recognition accuracy using JPEG2000 RoI coding. In M. Tistarelli and M. Nixon, editors, *Proceedings of the 3rd International Conference on Biometrics 2009 (ICB'09)*, volume 5558 of *LNCS*, pages 1102–1111. Springer Verlag, 2009.

[10] H. Hofbauer, F. Alonso-Fernandez, P. Wild, J. Bigun, and A. Uhl. A ground truth for iris segmentation. In *Proceedings of the 22th International Conference on Pattern Recognition (ICPR'14)*, page 6pp., Stockholm, Sweden, 2014.

[11] K. Horvath, H. Stögner, and A. Uhl. Effects of JPEG XR compression settings on iris recognition systems. In P. Real, D. Diaz-Pernil, H. Molina-Abril, A. Berciano, and W. Kropatsch, editors, *Proceedings of the 14th International Conference on Computer Analysis of Images and Patterns (CAIP 2011)*, volume 6855 of *LNCS*, pages 73–80. Springer Verlag, 2011.

[12] R. W. Ives, D. Bishop, Y. Du, and C. Belcher. Iris recognition: The consequences of image compression. *EURASIP Journal of Advances in Signal Processing*, 2010:Article ID 680845, doi:10.1155/2010/680845, 2010.

[13] R. W. Ives, R. P. Broussard, L. R. Kennell, and D. L. Soldan. Effects of image compression on iris recognition system performance. *Journal of Electronic Imaging*, 17:011015, doi:10.1117/1.2891313, 2008.

[14] M. Konrad, H. Stögner, and A. Uhl. Custom design of JPEG quantization tables for compressing iris polar images to improve recognition accuracy. In M. Tistarelli and M. Nixon, editors, *Proceedings of the 3rd Internat. Conference on Biometrics 2009 (ICB'09)*, volume 5558 of *LNCS*, pages 1091–1101. Springer Verlag, 2009.

[15] B. Kumar and G. Karpagam. An empirical analysis of requantization errors for recompressed jpeg images. *International Journal of Engineering Science and Technology*, 3(12):8519–8527, 2011.

[16] X. M. L. Zhang, L. Zhang. Rfsim: A feature based image quality asesment metric using riesz transforms. *Proc. 17th IEEE Int. Conf. on Image Procesing ICIP*, page p. 321?324, 2010. Hong Kong, China.

[17] S. Matschitsch, M. Tschinder, and A. Uhl. Comparison of compression algorithms' impact on iris recognition accuracy. In S.-W. Lee and S. Li, editors, *Proceedings of the 2nd International Conference on Biometrics 2007 (ICB'07)*, volume 4642 of *LNCS*, pages 232–241. Springer Verlag, 2007.

[18] B. Pardamean and I. Christiani. Comparatative evaluation of iris recognition performance. *International Journal of Mathematical Models and Methods in Applied Sciences*, 6(2):332–339, 2012.

[19] W. Pennebaker and J. Mitchell. *JPEG – Still image compression standard*. Van Nostrand Reinhold, New York, 1993.

[20] P. Philips, K. Bowyer, and P. Flynn. Comments on the CASIA version 1.0 iris data set. *IEEE Transactions on Pattern Analysis and Machine Intelligence*, 29(10):1869–1870, Oct. 2007.

[21] S. Rakshit and D. Monro. An evaluation of image sampling and compression for human iris recognition. *IEEE Transactions on Information Forensics and Security*, 2(3):605–612, 2007.

[22] C. Rathgeb, A. Uhl, and P. Wild. *Iris Recognition: From Segmentation to Template Security*, volume 59 of *Advances in Information Security*. Springer Verlag, 2013.

[23] C. Rathgeb, A. Uhl, and P. Wild. Effects of severe image compression on iris segmentation performance. In *IJCB 2014*, September 2014.

[24] H. Sencar and N. Memon. *Digital Image Forensics: There is more to a picture than meets the eye*. Springer Verlag, 2012.

[25] A. Tuba, J. Arezina, and R. Jovanovic. Software framework for testing JPEG quantization tables for iris recognition. In *Applied Mathematics in Electrical and Computer Engineering*, pages 417–422, 2012.

[26] Z. Wang, E. P. Simoncelli, and A. C. Bovik. Multi-scale structural similarity for image quality assessment. *IEEE Asiloma Conference on Signal, Systems and Computers*, 2003.